bioRxiv preprint doi: https://doi.org/10.1101/2020.07.10.197624; this version posted January 26, 2021. The copyright holder for this preprint (which was not certified by peer review) is the author/funder, who has granted bioRxiv a license to display the preprint in perpetuity. It is made available under aCC-BY-NC-ND 4.0 International license.

Classification: Biological Sciences; Evolution

Geography is more important than life history in the recent diversification of the tiger salamander complex

Kathryn M. Everson[a,1], Levi N. Gray[a,1], Angela G. Jones[a], Nicolette M. Lawrence[a], Mary E. Foley[a], Kelly L. Sovacool[a,b], Justin D. Kratovil[a,c], Scott Hotaling[a,d], Paul M. Hime[a,e], Andrew Storfer[d], Gabriela Parra-Olea[f], Ruth Percino-Daniel[g], X. Aguilar-Miguel[h], Eric M. O'Neill[a], Luis Zambrano[f], H. Bradley Shaffer[i], David W. Weisrock[a,2]

[a] Department of Biology, University of Kentucky, Lexington, KY 40506 USA

[b] Department of Computational Medicine & Bioinformatics, University of Michigan, Ann Arbor, MI 48109 USA

[c] Ecology and Evolutionary Biology Department, University of Connecticut, Storrs, CT 06269 USA

[d] School of Biological Sciences, Washington State University, Pullman, WA 99164 USA

[e] Biodiversity Institute, University of Kansas, Lawrence, KS 66045 USA

[f] Departamento de Zoología, Instituto de Biología, Universidad Nacional Autónoma de México, Ciudad Universitaria, Coyoacán, Ciudad de México 04510, México

[g] Departamento de Ecología Evolutiva, Instituto de Ecología, Universidad Nacional Autónoma de México, Ciudad Universitaria, Coyoacán, Ciudad de México 04510, México

[h] CIRB, Facultad de Ciencias, Universidad Autónoma del Estado de México, Toluca 50000, Edo. de México, México

bioRxiv preprint doi: https://doi.org/10.1101/2020.07.10.197624; this version posted January 26, 2021. The copyright holder for this preprint (which was not certified by peer review) is the author/funder, who has granted bioRxiv a license to display the preprint in perpetuity. It is made available under aCC-BY-NC-ND 4.0 International license.

[i] Department of Ecology and Evolutionary Biology, and La Kretz Center for California Conservation Science, University of California, Los Angeles, CA 90095 USA

[1] K.M.E. and L.N.G. contributed equally to this work

[2] To whom correspondence may be addressed. Email: david.weisrock@uky.edu

bioRxiv preprint doi: https://doi.org/10.1101/2020.07.10.197624; this version posted January 26, 2021. The copyright holder for this preprint (which was not certified by peer review) is the author/funder, who has granted bioRxiv a license to display the preprint in perpetuity. It is made available under aCC-BY-NC-ND 4.0 International license.

ABSTRACT

The North American tiger salamander species complex, including its best-known species, the Mexican axolotl, has long been a source of biological fascination. The complex exhibits a wide range of variation in developmental life history strategies, including populations and individuals that undergo metamorphosis, those able to forego metamorphosis and retain a larval, aquatic lifestyle (i.e., paedomorphosis), and those that do both. This life history variation has been assumed to lead to reproductive isolation and speciation, but the degree to which it has shaped population- and species-level divergence is poorly understood. Using a large multi-locus dataset from hundreds of samples across North America, we identified genetic clusters across the geographic range of the tiger salamander complex. These clusters often contain a mixture of paedomorphic and metamorphic taxa, indicating that geographic isolation has played a larger role in lineage divergence than paedomorphosis in this system. This conclusion is bolstered by geography-informed analyses indicating no effect of life history strategy on population genetic differentiation and by model-based analyses demonstrating gene flow between adjacent metamorphic and paedomorphic populations. This fine-scale genetic perspective on life-history variation establishes a framework for understanding how plasticity, local adaptation, and gene flow contribute to lineage divergence. Many members of the tiger salamander complex are endangered, and the Mexican axolotl is an important model system in regenerative and biomedical research. Our results chart a course for more informed use of these taxa in experimental, ecological, and conservation research.

Keywords: *Ambystoma*, life history, phylogenetics, population genomics, salamanders

bioRxiv preprint doi: https://doi.org/10.1101/2020.07.10.197624; this version posted January 26, 2021. The copyright holder for this preprint (which was not certified by peer review) is the author/funder, who has granted bioRxiv a license to display the preprint in perpetuity. It is made available under aCC-BY-NC-ND 4.0 International license.

SIGNIFICANCE STATEMENT

Population structure and speciation are shaped by a combination of biotic and abiotic factors. The tiger salamander complex has been considered to be a key group where life history variation has led to a rapid rate of speciation, driven in large part by the evolution of obligate paedomorphosis–a condition where adults maintain an aquatic, larval phenotype. Using a large multi-locus dataset, we present evidence of gene flow between taxa with different life history strategies, suggesting that obligate paedomorphosis is not a strong driver of speciation in the tiger salamander complex. Many of these nominal taxa are listed as critically endangered, and our genetic results provide information and guidance that will be useful for their conservation.

bioRxiv preprint doi: https://doi.org/10.1101/2020.07.10.197624; this version posted January 26, 2021. The copyright holder for this preprint (which was not certified by peer review) is the author/funder, who has granted bioRxiv a license to display the preprint in perpetuity. It is made available under aCC-BY-NC-ND 4.0 International license.

Introduction

Life history—the complement of traits affecting survival and reproduction over an organism's lifetime—affects ecology and dispersal, and therefore plays a potentially important role in shaping population structure and speciation (1, 2). The Mexican axolotl (*Ambystoma mexicanum*; hereafter, "axolotl") and related salamander species of the North American *Ambystoma tigrinum* complex (Table 1) display enormous life history variation, particularly with respect to the completion of metamorphosis (3). Some species are considered obligate paedomorphs, where sexually mature adults retain a larval, aquatic body plan that includes external gills and an enlarged tail fin (4). Others are considered obligate metamorphs, transforming from aquatic larvae to terrestrial juveniles, eventually returning to the water to breed as adults. Most populations are facultative, transforming under certain genetic and/or environmental conditions (5–8). This lability in life history is believed to have played an important role in the diversification of the *A. tigrinum* complex, particularly in the Trans-Mexican Volcanic Belt (TMVB) region, where several paedomorphic species, including the axolotl, are currently recognized (9–11). Obligate paedomorphosis is estimated to have evolved in this region multiple times (11–13) in association with relatively large, permanent bodies of water. Presumably, restricted gene flow between these isolated, paedomorphic populations led to speciation as well as morphological adaptations to the aquatic lifestyle (14).

The term "species complex," while not a formal taxonomic category, is often used to describe groups of closely related lineages early in the divergence process. The tiger salamander species complex has been highlighted as a potentially valuable example of such a recent radiation (15) that could provide insight into the early mechanisms initiating and/or maintaining diversity (16–21). However, species complexes pose a number of challenges: phenotypic

bioRxiv preprint doi: https://doi.org/10.1101/2020.07.10.197624; this version posted January 26, 2021. The copyright holder for this preprint (which was not certified by peer review) is the author/funder, who has granted bioRxiv a license to display the preprint in perpetuity. It is made available under aCC-BY-NC-ND 4.0 International license.

differences among lineages may be subtle or absent (i.e., cryptic species), ancestral polymorphisms may lead to incomplete lineage sorting that confounds molecular systematic studies, and reproductive barriers may be incomplete. The reliance on phenotype for species diagnosis in the *A. tigrinum* complex may require particular scrutiny, as several phenotypic traits, including developmental state and adult color pattern, can be plastic and highly variable (22–24). Given these challenges, fundamental questions remain concerning the reality of component lineages within the tiger salamander complex, calling into question the current taxonomy as an accurate reflection of its underlying evolutionary history.

Previous research has produced mixed results regarding levels of genetic differentiation among lineages in the *A. tigrinum* complex, as well as the relative importance of paedomorphosis as a driver of diversification. While population- and species-level structure is evident, an important theme emerging across multiple studies has been that reproductive barriers are porous (11, 25, 26). Shaffer and McKnight (11) noted "the striking lack of differentiation among the 14 species of the tiger salamander complex" (p. 425). Some studies have found an elevated degree of population structure among paedomorphic populations relative to metamorphic populations (12, 27). However, others have shown a lack of effect of paedomorphosis on population genetic differentiation (28), and demonstrated that paedomorphic taxa and neighboring metamorphic populations interbreed (29). Furthermore, crosses between metamorphic and paedomorphic taxa can produce viable hybrid offspring under laboratory conditions (30, 31).

To understand the processes underlying diversification in the tiger salamander complex, an important first step must be a range-wide assessment of population structure and the clarification of population- and species-level boundaries. With this groundwork, insights into the role of paedomorphosis and diversification can be addressed. For a study system of this

bioRxiv preprint doi: https://doi.org/10.1101/2020.07.10.197624; this version posted January 26, 2021. The copyright holder for this preprint (which was not certified by peer review) is the author/funder, who has granted bioRxiv a license to display the preprint in perpetuity. It is made available under aCC-BY-NC-ND 4.0 International license.

109 geographic and taxonomic scale, robust inference of population structure requires information
110 from multiple genes combined with thorough range-wide sampling. To meet these criteria, we
111 expand on a large multi-locus dataset containing 95 nuclear loci for 93 individuals (32), to
112 produce a data matrix for 347 individuals across the full geographic range of tiger salamanders
113 (Fig. S1). Given the complex and somewhat checkered history of the group's taxonomy, we
114 focus on a naïve approach, performing population structure analyses without *a priori*
115 identification of taxa to resolve geographic genetic clusters and characterize patterns of
116 admixture. We also overlay these results on the existing taxonomy to explore the correspondence
117 between current taxonomy and genetic differentiation. We then use these data for a phylogenetic
118 analysis to provide an updated working hypothesis for the evolution of the group. Finally, we test
119 the hypothesis that life history evolution has driven speciation in the tiger salamander complex,
120 particularly through the assumed isolation of paedomorphic species. In light of the life history
121 variation in this species complex, we use natural history information to place taxa into one of
122 five categories (Table 1) reflecting their propensity to metamorphose, then use model-based tests
123 of migration to ask whether paedomorphic populations (categories 4 and 5) exhibit greater levels
124 of genetic differentiation relative to those that regularly metamorphose (categories 1-3).
125

126 **RESULTS AND DISCUSSION**

127 *Identification of genetic lineages and phylogenetic relationships*

128 A principal components analysis (PCA) and a discriminant analysis of principal
129 components (DAPC; 33) both recovered *Ambystoma californiense* Gray 1853 as genetically
130 distinct from all other tiger salamanders (Fig. 1A, S2, S3), consistent with previous work (e.g.,
131 11, 34). Given that *A. californiense* is the only obligate metamorph in the complex (life history

bioRxiv preprint doi: https://doi.org/10.1101/2020.07.10.197624; this version posted January 26, 2021. The copyright holder for this preprint (which was not certified by peer review) is the author/funder, who has granted bioRxiv a license to display the preprint in perpetuity. It is made available under aCC-BY-NC-ND 4.0 International license.

category 1; Table 1) and is genetically divergent and geographically isolated from all other tiger salamanders evaluated in this study, we focus the remaining analyses on the other members of the complex. After removing *A. californiense* from the dataset, DAPC supported the recognition of three primary genetic clusters: U.S. (including samples from southern Canada), northwestern Mexico (primarily the Sierra Madre Occidental), and the central Mexican highlands (Fig. 1B, S4). A PCA of these data produced similar clustering results, with ordination patterns largely mirroring geographic sampling (Fig. S5). For a further discussion of the taxonomic implications of our results, see the Supplementary Material.

Within central Mexico, we identified $K = 7$ as the best-fit number of clusters in both DAPC and STRUCTURE analyses (Figs. 2A, S6). However, several of these clusters were only represented as a small proportion of genetic assignments, rather than as meaningful groups of individuals, and visual inspection at multiple levels of K revealed four clear geographic clusters (hereafter referred to as CM1-CM4) that captured the primary patterns of genetic differentiation and admixture across this region (Figs. 2A, S7-S8). Network analysis (35) also recovered groups that generally correspond to CM1-CM4, but with evidence of many reticulations (Fig. 3). This starburst-like pattern indicates the presence of conflicting topologies within the dataset (35), which can be caused by biological processes including recent diversification with incomplete lineage sorting, current or evolutionarily recent gene flow, or both. Phylogenetic analyses (36–38) recovered monophyletic CM1, CM2, and CM4 clusters (see below for discussion of CM3), but often with low statistical support (Fig. 3).

Based on type locality and range information, the CM1 cluster includes three stream-breeding and facultatively paedomorphic taxa: *Ambystoma altamirani* Dugès 1895 (39), *A. leorae* (Taylor 1943) (40), and *A. rivulare* (Taylor 1940) (9). Subsequent analyses of this cluster

bioRxiv preprint doi: https://doi.org/10.1101/2020.07.10.197624; this version posted January 26, 2021. The copyright holder for this preprint (which was not certified by peer review) is the author/funder, who has granted bioRxiv a license to display the preprint in perpetuity. It is made available under aCC-BY-NC-ND 4.0 International license.

identified two admixed populations associated with eastern and western portions of its geographic distribution (Figs. 2B, S9). Phylogenetically, CM1 was monophyletic and sister to all other central Mexican groups (Fig. 3).

CM2 grouped *A. lermaense* (Taylor 1940) (9) with samples corresponding to the type localities and range of *A. bombypellum* Taylor 1940 (9) and *A. granulosum* Taylor 1944 (41). There was no evidence for genetic isolation among any of these three taxa (Figs. 2C, S9).

Within CM3, population-genetic analyses first separated samples of *A. ordinarium* Taylor 1940 (5) from the rest (with no admixture detected; Figs. 2D, S9). Other samples clustered into northern and southern groups with some admixture in intermediate localities. The more southern cluster includes two obligately paedomorphic (category 5) taxa, *A. andersoni* Krebs & Brandon 1984 (42) and *A. dumerilii* (Dugès 1870) (43), endemic to Lakes Zacapú and Pátzcuaro, respectively. The samples from other CM3 localities likely represent what are currently classified as *A. amblycephalum* Taylor 1940 (9) and *A. flavipiperatum* Dixon 1963 (44).

CM4 included the axolotl, *A. mexicanum* (Shaw & Nodder 1798) (45), and *A. taylori* Brandon et al. 1981 (10)—both category 4 paedomorphs—as well as samples assigned to the facultatively paedomorphic (category 3) *A. velasci* (Duges 1888) (46). Subsequent DAPC and STRUCTURE analyses of CM4 placed all but one *A. mexicanum* individual sampled from Lakes Xochimilco and Chapultepec (i.e., the remaining habitats of the axolotl) in a distinct cluster (Fig. 2E, S9), with evidence of some admixture in samples to the northwest of Mexico City.

Within the U.S. and Canada (excluding *A. californiense)*, DAPC and STRUCTURE identified three genetic clusters ($K = 3$), with clear signs of admixed contact zones (Figs. 2F, S10, S11). Geographically, these clusters are associated with the eastern U.S., the central + western U.S., and the southwestern U.S. + Rocky Mountains (hereafter, we refer to the latter two

bioRxiv preprint doi: https://doi.org/10.1101/2020.07.10.197624; this version posted January 26, 2021. The copyright holder for this preprint (which was not certified by peer review) is the author/funder, who has granted bioRxiv a license to display the preprint in perpetuity. It is made available under aCC-BY-NC-ND 4.0 International license.

178 groups as central U.S. and Rocky Mountain U.S., respectively). Populations in the eastern U.S.
179 are assignable to *A. tigrinum* Green 1825, while central U.S. and Rocky Mountain U.S.
180 populations to *A. mavortium* Baird 1850. Phylogenetic analyses corroborated these results, albeit
181 with extensive reticulations among clusters in the phylogenetic network (Fig. 3) and mixed
182 support for species-tree relationships among the three major groups (Fig. 3 vs. Fig. S13). Further
183 exploration of population structure within each of the three U.S. clusters recovered additional
184 patterns of differentiation (Figs. S10, S11), including northern and southern clusters in the
185 eastern U.S. and central U.S., and an allopatric cluster restricted to the Pacific Northwest.
186 Overall, our U.S. results are similar to mtDNA-based results from previous studies, which
187 identified haplotype clades associated with the eastern U.S., Great Plains and Rocky Mountains,
188 and the Pacific Northwest (11, 47).
189 All analyses of the northern Mexico group identified two genetic clusters ($K = 2$; Figs.
190 2G, S12). The northern cluster corresponds to *A. rosaceum* Taylor 1941 (48), while the southern
191 cluster is likely *A. silvense* Webb 2004 (49, see also 50). Phylogenetic analyses recovered each
192 of these two northern Mexico clusters as monophyletic, but not sister to one another, and with
193 few reticulate nodes in the phylogenetic network (Fig. 3, S13).
194
195 *Does paedomorphosis lead to increased genetic differentiation?*
196 As a first step in addressing this question, we used Bayesian modeling to test for genetic
197 isolation of paedomorphic taxa (i.e., species scored as life history category 4 or 5 in Table 1). We
198 tested for gene flow between paedomorphs–*A. andersoni* and *A. dumerilii* in CM3, and *A.*
199 *mexicanum* and *A. taylori* in CM4–and their surrounding facultatively paedomorphic
200 populations. For both CM3 and CM4, the top-ranking models included migration among all

bioRxiv preprint doi: https://doi.org/10.1101/2020.07.10.197624; this version posted January 26, 2021. The copyright holder for this preprint (which was not certified by peer review) is the author/funder, who has granted bioRxiv a license to display the preprint in perpetuity. It is made available under aCC-BY-NC-ND 4.0 International license.

populations, regardless of their degree of paedomorphosis (Fig. 4). Alternative models of no migration or restricted migration (Fig. S14) were rejected with decisive Bayes factors (Table S3). In CM3, migration rates entering the *A. dumerilii* population were higher than those leaving that population, while migration rates entering and exiting *A. andersoni* were approximately equal. In CM4, migration rates exiting the *A. mexicanum* population were much higher than those entering the population while migration rates entering and exiting *A. taylori* were approximately equal (Fig. 4, Table S4). An important caveat to our migration and population structure analyses is that divergence time is not included as a model parameter, which prevents distinguishing between historical and contemporary gene flow. Thus, our ability to differentiate ongoing from historical gene flow in these tests is limited.

We also assessed whether a paedomorphic life history is associated with greater population genetic differentiation (calculated here as Φ_{ST}), which would be expected if paedomorphosis is an important reproductive barrier (12). Plots of Φ_{ST} against geographic distance showed that comparisons involving paedomorphic populations were largely overlapping with those based on facultative-facultative comparisons, with no difference in slope or y-intercept (Fig. 4). In both CM3 and CM4, partial Mantel tests found no significant correlation between life history and pairwise Φ_{ST} after correcting for geographic distance (Fig. 4).

The influence of life history on diversification

A popular perspective on diversification in this species complex is that paedomorphosis promotes reproductive isolation and, ultimately, speciation (10, 11). An important theme of our results is that taxa with different life history strategies commonly cluster together by geography in population genetic and phylogeographic analyses (Figs. 2, 3). Furthermore, genetic

bioRxiv preprint doi: https://doi.org/10.1101/2020.07.10.197624; this version posted January 26, 2021. The copyright holder for this preprint (which was not certified by peer review) is the author/funder, who has granted bioRxiv a license to display the preprint in perpetuity. It is made available under aCC-BY-NC-ND 4.0 International license.

differentiation is not significantly greater for paedomorphic populations, relative to facultative populations, and there has been substantial gene flow among populations with different life history strategies (Fig. 4). Thus, the evolution of life history extremes does not appear to be the main driver of speciation in the tiger salamander complex.

It is also worth noting that facultative paedomorphosis is the inferred ancestral condition (8) and nearly all extant lineages in the *Ambystoma tigrinum* complex are capable of metamorphosis, either in the wild or in the lab. Only *A. dumerilii* is not known to survive metamorphosis, even under laboratory conditions (51). That only one described taxon in the complex is demonstrably fixed for paedomorphosis raises several questions: Are the rest of the primarily paedomorphic populations *en route* to fixation, rather than actually fixed? Have lineages fixed for paedomorphosis gone extinct? Do facultative populations fluctuate in paedomorph frequency over time, depending on environmental and/or demographic conditions (5)? Do transforming and non-transforming individuals interbreed in nature? While these remain open questions, below we provide some relevant context for exploration and future research.

Theory predicts that paedomorphosis in salamanders is most likely to become fixed in a population when ecological conditions are favorable in the larval, aquatic environment but unfavorable on land (e.g., when terrestrial habitats are arid or resource-limited) (12, 52, 53). However, it is not known how long fixed populations persist over evolutionary time; obligate paedomorphic lineages may have arisen and gone extinct multiple times over tiger salamander evolutionary history (54). One situation that would result in complete speciation is if paedomorphosis became fixed in the population and migration with surrounding facultatively paedomorphic populations ceased due to strong assortative mating and/or selection against hybrids (55–57). However, assortative mating within life history morphs has not been

bioRxiv preprint doi: https://doi.org/10.1101/2020.07.10.197624; this version posted January 26, 2021. The copyright holder for this preprint (which was not certified by peer review) is the author/funder, who has granted bioRxiv a license to display the preprint in perpetuity. It is made available under aCC-BY-NC-ND 4.0 International license.

247 demonstrated in other salamanders (58–60) and different tiger salamander morphs can interbreed
248 (61). In fact, the only known instance of positive assortative mating in *A. tigrinum* is associated
249 with tail length (62, 63), which might favor metamorphosed males as paedomorphic individuals
250 can have relatively short tails (42). The evidence for selection against intermorph offspring is
251 also scarce. Captive breeding using artificial fertilization has produced *A. mexicanum* x *A.*
252 *tigrinum*, *A. dumerilii* x *A. tigrinum*, *A. andersoni* x *A. tigrinum*, and *A. dumerilii* x *A. rivulare*
253 hybrids (7, 31, 64–66). This suggests that postzygotic barriers are weak, although the extent to
254 which divergent lineages would interbreed in the wild remains a key question in need of
255 investigation.

256 If biological barriers to reproduction are limited or absent, there are several potential
257 mechanisms by which dispersal could mediate gene flow between paedomorphic and
258 metamorphic populations. First, metamorphosed individuals from facultatively paedomorphic
259 populations could move into bodies of water containing paedomorphic populations. Our
260 demographic analyses support this scenario, as they recovered immigration from facultative into
261 paedomorphic populations (Fig. 4). However, demographic analyses also estimated emigration
262 out of paedomorphic populations; thus, "obligate" paedomorphs might also occasionally
263 metamorphose and disperse. Occasional metamorphosis has been documented in several
264 putatively paedomorphic populations (9, 10, 42, 67–69), and may be more prevalent than
265 currently recognized because rare transformed individuals in nature are virtually impossible to
266 verify (70). Importantly, even a low frequency of transformed adults is likely sufficient to
267 maintain evolutionary cohesion with surrounding populations (10, 29, 71). Alternatively, the
268 dispersal of paedomorphs might be human-mediated; this could partially explain the elevated
269 emigration rates we observed in the axolotl (Fig. 4). Axolotls are known to be sold in local

bioRxiv preprint doi: https://doi.org/10.1101/2020.07.10.197624; this version posted January 26, 2021. The copyright holder for this preprint (which was not certified by peer review) is the author/funder, who has granted bioRxiv a license to display the preprint in perpetuity. It is made available under aCC-BY-NC-ND 4.0 International license.

markets as food, bait, or aquarium pets, and are sometimes moved from one area of central Mexico to another (72). Finally, gene flow may not necessarily be mediated across a terrestrial environment; genetic connectivity could also be maintained if populations have been forced into contact by water level fluctuations in the groundwater system of a region. The dynamic lacustrine history of the Cuenca Oriental (73), for instance, suggests that isolation of some paedomorphic populations has been punctuated by broader aquatic connections over short geological time scales, potentially facilitating gene flow. Collectively, these mechanisms may explain the maintenance of geographic genetic groups, now or in the evolutionarily recent past, containing a range of life histories.

The genetic cohesion we detected across wide swaths of the TMVB is particularly striking given other evidence for local adaptation in this region. This scenario is perhaps best exemplified in the Cuenca Oriental (Fig. 2E), where some lakes contain paedomorphic salamanders adapted to saline conditions, a very rare trait among amphibians (74). At one site, the saline Lake Alchichica, the population is currently considered a distinct species (*A. taylori*) (10). However, our results indicate that *A. taylori* is not genetically distinct from surrounding, putatively non-saline-adapted populations, a result consistent with a previous microsatellite-based study that found significant gene flow to and from *A. taylori* (29). While we cannot rule out the potential for localized selection and adaptation in the *A. taylori* genome, our results highlight that even populations adapted to aquatic conditions intolerable to most other *Ambystoma* have not reached a level of isolation identifying them as an independent evolutionary lineage (75).

bioRxiv preprint doi: https://doi.org/10.1101/2020.07.10.197624; this version posted January 26, 2021. The copyright holder for this preprint (which was not certified by peer review) is the author/funder, who has granted bioRxiv a license to display the preprint in perpetuity. It is made available under aCC-BY-NC-ND 4.0 International license.

Comparisons to previous work

This study included extensive geographic sampling of the tiger salamander complex, which provided a broad spatial context to more fully understand patterns of genetic variation. However, it is important to consider the possibility that our data are simply not sensitive enough to detect genetic differentiation associated with lineage divergence on an extremely recent time scale. The common ancestor of *A. californiense* and the remainder of the species complex dates to approximately five million years (11, 34), and phylogenomic data indicate that speciation across the remaining tiger salamander lineages occurred within the last one million years (76). Such recent timing renders lineage boundaries difficult to detect (15). Our markers, developed from transcriptomic resources (32), may not have an overall substitution rate sufficient to detect such subtle genetic differentiation. We recommend that future research uses a larger genomic dataset or faster-evolving loci with particular focus on the sampling of paedomorphs in this system. To this point, perhaps the strongest evidence for the genetic divergence of paedomorphic populations comes from past microsatellite-based work indicating the genetic distinctiveness of *A. andersoni* and *A. mexicanum* from a select set of populations across central Mexico (27) and the genetic distinctiveness of *A. taylori* from neighboring populations in the Cuenca Oriental (29). Both of these studies recovered signatures of gene flow, but identified greater overall population structure compared to this study, which could be due to numerous factors, including a faster microsatellite mutation rate and more limited locality sampling.

CONCLUSIONS

The extent to which populations within the tiger salamander complex exhibit phenotypic plasticity in life history traits is remarkable and is believed to have played a role in the rapid

bioRxiv preprint doi: https://doi.org/10.1101/2020.07.10.197624; this version posted January 26, 2021. The copyright holder for this preprint (which was not certified by peer review) is the author/funder, who has granted bioRxiv a license to display the preprint in perpetuity. It is made available under aCC-BY-NC-ND 4.0 International license.

accumulation of lineages observed in the highlands of central Mexico (11, 57). While our results suggest there is less species-level diversity in central Mexico than previously recognized, there is clearly more diversity in this region compared to the US and Canada where there is (a) more geographic space and (b) less life history variation within and between lineages. While we cannot fully explain the greater diversity in central Mexico, our results suggest that major patterns of diversification are related to a complex history of geographic isolation and secondary contact, in which life history strategy has played a less important role, at least in the long (evolutionary) run. We agree with previous work (12) that the complex geological history of the TMVB, including montane uplift and fluctuating drainage connectivity since the Miocene, has been the cornerstone of the evolutionary history of this species complex, and that the influences of geographic isolation and paedomorphosis may work synergistically to lead to the establishment of isolated populations. Lingering questions notwithstanding, this large-scale genetic and geographic study establishes a framework for understanding the evolutionary history of the *Ambystoma tigrinum* species complex. The results presented here will facilitate comparative studies of the axolotl and its allies, provide direction for conservation prioritization and management, and strengthen the use of the tiger salamander species complex as a model system in biology.

MATERIALS & METHODS

Geographic sampling

We generated new data from 254 individuals sampled from across the range of the *A. tigrinum* complex (Fig. S1; Table S1). These individuals were combined with 93 individuals sampled in O'Neill et al. (32) to produce a data set comprising 347 individuals. We sampled a

bioRxiv preprint doi: https://doi.org/10.1101/2020.07.10.197624; this version posted January 26, 2021. The copyright holder for this preprint (which was not certified by peer review) is the author/funder, who has granted bioRxiv a license to display the preprint in perpetuity. It is made available under aCC-BY-NC-ND 4.0 International license.

large number of localities (188) with 1-9 individuals sampled per locality (mean = 1.8). This sampling included 166 individuals from the US, 2 from Canada, and 178 from Mexico. *Ambystoma californiense* samples were primarily included as a close outgroup to the remainder of the species complex and were sampled from localities with limited to no impacts of introgression from invasive *A. mavortium* (47). Additional outgroup data were generated for two species outside of the *A. tigrinum* complex: *A. opacum* and *A. texanum*. Full details regarding the generation of these data can be found in the Supplementary Materials. All *A. tigrinum* complex species were assigned to a life history category based on review of the published literature and private field records from authors of this study. These life history categories are as follow: 1 = obligate metamorph (no paedomorphs have been documented in the field); 2 = strong bias towards metamorphosis with rare paedomorphs found in the field; 3 = both metamorphosis and paedomorphosis common in the field; 4 = strong bias towards paedomorphosis with rare metamorphs found in the field; 5 = obligate paedomorph (no metamorphs have been documented in the field). In the text, "paedomorph" describes taxa scored as 4 or 5, while "facultative paedomorph" describes taxa scored as 2 or 3.

Data collection and sequencing

We generated DNA sequence data from a panel of 95 nuclear loci developed specifically for the tiger salamander species complex. A more complete description of marker development can be found in O'Neill et al. (32). Genomic DNA was extracted using a DNeasy Blood and Tissue kit (Qiagen). For a small number of DNA extractions, we increased DNA quantities using a Repli-g whole genome amplification kit (Qiagen). We used an initial round of PCR in 96-well plate format to amplify all loci from an individual, followed by a smaller second round of PCR to

bioRxiv preprint doi: https://doi.org/10.1101/2020.07.10.197624; this version posted January 26, 2021. The copyright holder for this preprint (which was not certified by peer review) is the author/funder, who has granted bioRxiv a license to display the preprint in perpetuity. It is made available under aCC-BY-NC-ND 4.0 International license.

amplify loci that did not amplify in the initial PCR. See O'Neill et al. (32) for the details of PCR conditions and primer sequences.

PCR products from all loci were pooled for each individual in roughly equal concentrations based on the intensity of amplification as visualized on an agarose gel. Indexed Illumina sequencing libraries were generated for each individual using an Illumina Nextera XT DNA Library Preparation Kit (Illumina). Subsequent to library preparation, indexed libraries were quantified using a Qubit Fluorometer, pooled in equimolar concentrations, and checked on an Agilent Bioanalyzer to assure proper fragmentation.

Sequencing was performed in four rounds using an Illumina MiSeq. We performed an initial round using a total of seven individuals to test the compatibility of the Illumina Nextera XT library kit with our PCR amplicons. Three subsequent rounds of library preparation and sequencing were performed on sets of 96 individuals each, and some individuals were sequenced in multiple rounds due to initially low read counts. All sequencing was performed with paired-end 150 bp reads. Overall, we generated a total of 29,426,894 PE reads across all newly sequenced individuals, with an average of 309,757 PE reads, 1,148X coverage, and 7.6% missing loci per individual (Table S2).

Bioinformatics and dataset generation

All sequence reads were processed using a newly developed bioinformatic pipeline written for this project (https://doi.org/10.5281/zenodo.3585970) that produces multiple sequence alignments for individual loci and genome-wide SNP matrices sampled from variable sites. This pipeline was developed using the Snakemake workflow management system (77), linking together multiple software tools to take sequence data from raw reads to phased sequence

bioRxiv preprint doi: https://doi.org/10.1101/2020.07.10.197624; this version posted January 26, 2021. The copyright holder for this preprint (which was not certified by peer review) is the author/funder, who has granted bioRxiv a license to display the preprint in perpetuity. It is made available under aCC-BY-NC-ND 4.0 International license.

384 alignments for each locus. Demultiplexed paired-end Illumina fastq files were used as input, with
385 separate forward and reverse read files for each individual. Sequence data were trimmed and
386 filtered in Trimmomatic (78) using a sliding window of 4 base-pairs and a minimum average
387 quality score of 15. Filtered sequence reads were then aligned to reference sequences from the
388 O'Neill et al. (2013) dataset (32); specifically, we used the clean sequences of an *A. ordinarium*
389 sample that had high coverage and low amounts of missing data. The resulting aligned contigs
390 were processed using SAMtools (79) to filter and prepare data for FreeBayes (80), which was
391 used to call variable sites. Variants were filtered with VCFTools (81) by removing indels and
392 setting a quality threshold of phred score > 20 and a minimum read depth of 30. The program
393 WhatsHap (82) was used to perform read-based phasing of the data for each locus x individual
394 contig. Finally, phased haplotypes from each individual (two copies, regardless of homo- or
395 heterozygosity) were combined into an alignment of all individuals using MAFFT with the
396 default auto parameter (83). We generated fasta files of SNPs using the SNP-sites program (84)
397 and created a SNP genotype matrix by sampling variable sites from a concatenated sequence
398 alignment of all loci. We identified three loci (E12G1, E6A11, and E7G8) as potential paralogs
399 based on high alignment error and high levels of heterozygosity for all individuals. These three
400 loci were excluded from all analyses.
401 Across the remaining 92 loci, alignment lengths ranged from 123 to 630 bp (avg. = 270
402 bp) with a total concatenated alignment of 24,788 bp. For the full dataset, including *A. texanum*
403 and *A. opacum* outgroups, single-locus alignments contained an average of 55 variable sites
404 (min. = 15, max. = 121) and an average of 41 parsimony informative sites (min. = 11, max. =
405 102). Population genetic analyses restricted to the *A. tigrinum* complex including *A.*

bioRxiv preprint doi: https://doi.org/10.1101/2020.07.10.197624; this version posted January 26, 2021. The copyright holder for this preprint (which was not certified by peer review) is the author/funder, who has granted bioRxiv a license to display the preprint in perpetuity. It is made available under aCC-BY-NC-ND 4.0 International license.

406 *californiense*—which were further filtered for non-biallelic SNPs and a minor allele count ≥ 3—
407 contained a total of 2,360 SNPs.
408
409 *Population structure and lineage discovery*
410 We developed hypotheses of population-level lineages across the range of the *A. tigrinum*
411 complex ignoring the existing taxonomy, starting with the identification of major geographic
412 patterns of differentiation, and then performing a recursive set of analyses on more
413 geographically restricted sets of individuals. In our initial round of analyses we used two non-
414 parametric methods: principal components analysis (PCA) and discriminant analysis of principal
415 components (DAPC) (33). While both analyses provide a multivariate summary of genetic data,
416 DAPC is also used to assess the fit of data to varying numbers of population clusters. These
417 analyses were applied to our full genotypic dataset including *A. californiense* and all remaining
418 individuals from the *A. tigrinum* complex. The PCA was calculated using the function 'prcomp'
419 in the R package stats (85), while the DAPC was calculated using the package adegenet (86).
420 The optimal number of principal components to retain for DAPC was identified using cross-
421 validation via the xvalDapc function with default parameter values. DAPC was performed
422 without prior assignment of individuals to groups across a range of cluster levels (K = 1-20). We
423 used two metrics to identify the best estimate of the primary splits in our data. First, we used the
424 Bayesian Information Criterion (BIC) calculated in the DAPC analysis to assess the fit of the
425 data to different levels of K. We note that the level of K with the absolute lowest BIC may not be
426 a better explanation of the data than a K with a slightly higher BIC (87); therefore, we applied
427 this measure for general guidance on a range of K that may describe the data well. We paired this
428 assessment with visualizations of the first and second principal components (Fig. S2, S5) and

bioRxiv preprint doi: https://doi.org/10.1101/2020.07.10.197624; this version posted January 26, 2021. The copyright holder for this preprint (which was not certified by peer review) is the author/funder, who has granted bioRxiv a license to display the preprint in perpetuity. It is made available under aCC-BY-NC-ND 4.0 International license.

DAPC ordination plots to identify the level of *K* at which similar clustering patterns could be observed with minimal change at successively higher levels of *K*. DAPC of the complete tiger salamander species complex identified a consistent pattern beginning at $K = 5$ for high differentiation of all *A. californiense* samples (Fig. S3). Further DAPC analysis with *A. californiense* removed identified a consistent pattern beginning at $K = 5$ for differentiation between clusters of populations from northern and central Mexico, and three clusters of U.S. populations (two from the Western U.S. and one from the Eastern U.S.; Fig. S4).

Using the clusters identified in the DAPC analysis of the total data set, we then used both DAPC and STRUCTURE v.2.3.4 (88) to analyze subsequent data sets comprising smaller numbers of individuals. Recursive rounds of DAPC analyses were stopped when BIC scores showed little improvement ($\Delta BIC < 2$) at values of $K > 1$. STRUCTURE analyses used an admixture model and 500,000 generations following a burn-in of 100,000 generations. Analyses were performed for $K = 1$-10 with 16 replicate analyses for each *K*. To help identify an optimal value for *K*, we calculated ΔK using the Evanno method (89) via the CLUMPAK web tool (90). A limitation of the Evanno method is that it cannot estimate the likelihood of $K = 1$ (89), thus, we also visually inspected individual group assignments and concluded a value of $K = 1$ if the corresponding DAPC cluster showed little improvement ($\Delta BIC < 2$) at values of $K > 1$, or when individuals were simply being split without any geographic or individual clustering. We also evaluated models where *K* was equal to the number of currently recognized species in that genetic cluster (e.g., $K = 3$ for CM1, which included the type localities for three described species: *A. altamirani*, *A. leorae*, and *A. rivulare*). We mapped individual species assignments onto these results to test the potential correspondence between naïve clustering and the existing taxonomy (Fig. S9).

bioRxiv preprint doi: https://doi.org/10.1101/2020.07.10.197624; this version posted January 26, 2021. The copyright holder for this preprint (which was not certified by peer review) is the author/funder, who has granted bioRxiv a license to display the preprint in perpetuity. It is made available under aCC-BY-NC-ND 4.0 International license.

452

453 *Phylogenetic reconstruction*

454 Given the high levels of admixture among groups, we used SplitsTree v. 4.14.8 (35, 91)
455 to generate four phylogenetic networks: one with all tiger salamander individuals, and one each
456 for the U.S., central Mexico, and northern Mexico subgroups. Networks were constructed using
457 uncorrected p-distances and the NeighborNet algorithm (92).

458 We also used three different analytical approaches to place hypothesized population
459 lineages in a phylogenetic framework. For all analyses we used a reduced data set containing the
460 concatenated data for 2-7 representative individuals from each population genetic cluster, which
461 limited computation time and avoided violating the coalescent-model assumption of zero gene
462 flow. We first inferred the phylogeny using Bayesian Inference in BEAST v.1.8.3 (37). Analyses
463 were run for 5 million generations, sampling every 1,000 generations after the first 500,000
464 generations were removed as burn-in. Run convergence was assessed with Tracer v.1.6.0 (93).
465 Next, we inferred a maximum-likelihood phylogeny using RAxML v.8 (38). Node support was
466 assessed using a rapid bootstrap analysis with 1,000 replicates, which was summarized as a 95%
467 rule consensus tree using the program SumTrees in the DendroPy python library (94). For both
468 BEAST and RAxML, PartitionFinder (95) was used to identify the number of preferred gene
469 partitions and their substitution models, and analyses were performed on the CIPRES Science
470 Gateway server (96). Finally, we inferred phylogenetic relationships using SVDquartets (36)
471 implemented in PAUP* version 4.0a164 (97), sampling all possible quartets and assessing node
472 support with 1,000 bootstrap replicates. For all phylogenetic analyses, trees were visualized
473 using FigTree v.1.4.2 (98).

bioRxiv preprint doi: https://doi.org/10.1101/2020.07.10.197624; this version posted January 26, 2021. The copyright holder for this preprint (which was not certified by peer review) is the author/funder, who has granted bioRxiv a license to display the preprint in perpetuity. It is made available under aCC-BY-NC-ND 4.0 International license.

474

475 *Tests of migration and population differentiation of paedomorphic taxa*

476 We used the coalescent-based program Migrate-N v.3.2 (99) to explicitly test for
477 population structure and gene flow in each obligately paedomorphic species of *Ambystoma* (*A.*
478 *andersoni, A. dumerilii, A. taylori,* and *A. mexicanum*). For each model (Fig. S14), we treated
479 paedomorphic species as distinct populations, and the facultatively paedomorphic individuals
480 from the same genetic cluster (CM3 or CM4) as another population. The best-fitting model was
481 determined via Bayes factors (BF), which were calculated using Bézier-corrected marginal
482 likelihoods (Table S3); the highest-ranking models have a BF = 0. Each Migrate-N analyses ran
483 for 50 million steps, recording every 10 steps, with a burn-in of five million and the default
484 heating scheme. Suitable upper bounds for priors on population size (Θ) and migration rate (*M*)
485 were determined from an initial test run of 10 million steps for each analysis. Median values and
486 95% confidence intervals of Θ and *M* are in Fig. 4 and Table S4.

487 Within CM3 and CM4, we also calculated pairwise Φ_{ST} (a metric of population
488 differentiation) among all populations using the function 'pairPhiST' in the R package
489 haplotypes (100). These values were plotted against pairwise geographic distances (Fig. 4),
490 which were calculated from locality latitude/longitude data (Table S1) and converted to
491 kilometers using the function 'rdist.earth' in the R package fields (101). A life history matrix was
492 also generated by assigning a value of 0 for pairwise comparisons of populations with the same
493 life history and a value of 1 for populations with different life histories (i.e., facultatively
494 paedomorphic vs. obligately paedomorphic). Paedomorph-paedomorph comparisons were
495 omitted to avoid confounding them with facultative-facultative comparisons. Finally, we used
496 these matrices in a partial mantel test [function 'mantel.partial' package vegan (102)] to test for a

bioRxiv preprint doi: https://doi.org/10.1101/2020.07.10.197624; this version posted January 26, 2021. The copyright holder for this preprint (which was not certified by peer review) is the author/funder, who has granted bioRxiv a license to display the preprint in perpetuity. It is made available under aCC-BY-NC-ND 4.0 International license.

497 correlation between Φ_{ST} and life history while correcting for geographic distance. Significance of
498 this test was determined using 999 permutations and an alpha level of 0.05.
499

500 **DATA AVAILABILITY**

501 Supplementary figures and tables are provided with the online version of this manuscript.
502 Input files for all population genetic and phylogenetic analyses are available via figshare
503 (https://figshare.com/projects/Life_history_strategy_does_not_reflect_genetic_differentiation_in
504 _the_tiger_salamander_species_complex/74115). Sequence data are available on the NCBI
505 Sequence Read Archive (BioProject accession PRJNA594660).
506

507 **ACKNOWLEDGEMENTS**

508 This project was supported by grants from the National Science Foundation [DEB-
509 0949532, DEB-1355000, and DEB-1406876 (DDIG awarded to J. D. Kratovil)] and by a
510 University Research Fellowship awarded to K. M. Everson from the University of Kentucky. We
511 thank Chris Beachy, Jim Bogart, Ken Carbale, Sheri Church, Jeff LeClere, Carol Hall, Paul
512 Moler, Nancy Staub, and Ken Wray for genetic samples, and Jose Bocanegra, Ben Browning,
513 Mackenzie Humphrey, Mary Virginia Gibbs, Ricky Grewelle, Alan Lemmon, Emily Moriarty
514 Lemmon, Deborah Lu, Stephanie Mitchell, Alex Noble, Tolu Odukoya, Ben Tuttle, and Josh
515 Williams for assistance with data collection and analyses.
516

bioRxiv preprint doi: https://doi.org/10.1101/2020.07.10.197624; this version posted January 26, 2021. The copyright holder for this preprint (which was not certified by peer review) is the author/funder, who has granted bioRxiv a license to display the preprint in perpetuity. It is made available under aCC-BY-NC-ND 4.0 International license.

REFERENCES

1. S. R. Palumbi, Marine speciation on a small planet. *Trends Ecol. Evol.* **7**, 114–118 (1992).
2. S. Mopper, S. Y. Strauss, *Genetic Structure and Local Adaptation in Natural Insect Populations: Effects of Ecology, Life History, and Behavior* (Springer US, 1998).
3. S. J. Gould, *Ontogeny and Phylogeny* (Harvard University Press, 1977).
4. D. B. Wake, Paedomorphosis. *J. Herpetol.* **14**, 80 (1980).
5. H. H. Whiteman, Evolution of facultative paedomorphosis in salamanders. *Q. Rev. Biol.* **69**, 205–221 (1994).
6. R. B. Page, *et al.*, Effect of thyroid hormone concentration on the transcriptional response underlying induced metamorphosis in the Mexican axolotl (*Ambystoma*). *BMC Genomics* **9**, 78 (2008).
7. S. R. Voss, Genetic Basis of Paedomorphosis in the Axolotl, *Ambystoma mexicanum*: A Test of the Single-Gene Hypothesis. *J. Hered.* **86**, 441–447 (1995).
8. S. R. Voss, H. B. Shaffer, Adaptive evolution via a major gene effect: paedomorphosis in the Mexican axolotl. *Proc. Natl. Acad. Sci. USA* **94**, 14185–9 (1997).
9. E. H. Taylor, New salamanders from Mexico with a discussion of certain known forms. *Univ. Kansas Sci. Bull.* **26**, 407–439 (1939).
10. R. Brandon, E. Maruska, W. Rumph, A new species of neotenic *Ambystoma* (Amphibia, Caudata) endemic to Laguna Alchichica, Puebla, Mexico. *Bull. South. Calif. Acad. Sci.* **80**, 112–125 (1981).
11. H. B. Shaffer, M. L. McKnight, The polytypic species revisited: Genetic differentiation and molecular phylogenetics of the tiger salamander *Ambystoma tigrinum* (Amphibia:

bioRxiv preprint doi: https://doi.org/10.1101/2020.07.10.197624; this version posted January 26, 2021. The copyright holder for this preprint (which was not certified by peer review) is the author/funder, who has granted bioRxiv a license to display the preprint in perpetuity. It is made available under aCC-BY-NC-ND 4.0 International license.

Caudata) complex. *Evolution* **50**, 417–433 (1996).

12. H. B. Shaffer, Evolution in a paedomorphic lineage. I. An electrophoretic analysis of the Mexican ambystomatid salamanders. *Evolution* **38**, 1194–1206 (1984).

13. H. B. Shaffer, Phylogenetics of model organisms: The laboratory axolotl, *Ambystoma Mexicanum*. *Syst. Biol.* **42**, 508–522 (1993).

14. H. B. Shaffer, Evolution in a paedomorphic lineage. II. Allometry and form in the Mexican ambystomatid salamanders. *Evolution* **38**, 1207–1218 (1984).

15. H. B. Shaffer, R. C. Thomson, Delimiting Species in Recent Radiations. *Syst. Biol.* **56**, 896–906 (2007).

16. P. R. Grant, Speciation and the adaptive radiation of Darwin's finches. *Am. Sci.* **69**, 653–663 (1981).

17. O. Seehausen, Explosive speciation rates and unusual species richness in haplochromine cichlid fishes: Effects of sexual selection. *Adv. Ecol. Res.* **31**, 237–274 (2000).

18. M. Fegan, P. Prior, "How complex is the *Ralstonia solanacearum* species complex" in *Bacterial Wilt Disease and the Ralstonia Solanacearum Species Complex*, C. Allen, P. Prior, A. C. Hayward, Eds. (American Phytopathological Society Press, 2005), pp. 449–461.

19. J. Mallet, Hybrid speciation. *Nature* **446**, 279–283 (2007).

20. M. C. Fontaine, *et al.*, Extensive introgression in a malaria vector species complex revealed by phylogenomics. *Science* **347**, 1258524 (2015).

21. J. Geml, G. A. Laursen, K. O'Neill, H. C. Nusbaum, D. L. Taylor, Beringian origins and cryptic speciation events in the fly agaric (*Amanita muscaria*). *Mol. Ecol.* **15**, 225–239 (2005).

bioRxiv preprint doi: https://doi.org/10.1101/2020.07.10.197624; this version posted January 26, 2021. The copyright holder for this preprint (which was not certified by peer review) is the author/funder, who has granted bioRxiv a license to display the preprint in perpetuity. It is made available under aCC-BY-NC-ND 4.0 International license.

563 22. R. Newman, Adaptive plasticity in amphibian metamorphosis. *Bioscience* **42**, 671–678
564 (1992).
565 23. H. H. Whiteman, S. A. Wissinger, W. S. Brown, Growth and foraging consequences of
566 facultative paedomorphosis in the tiger salamander, *Ambystoma tigrinum nebulosum*.
567 *Evol. Ecol.* **10**, 433–446 (1996).
568 24. P. J. Fernandez, J. P. Collins, Effect of environment and ontogeny on color pattern
569 variation in Arizona tiger salamanders (*Ambystoma tigrinum nebulosum* Hallowell).
570 *Copeia* **1988**, 928 (1988).
571 25. S. P. D. Riley, H. B. Shaffer, S. R. Voss, B. M. Fitzpatrick, Hybridization between a rare,
572 native tiger salamander (*Ambystoma californiense*) and its introduced congener. *Ecol.*
573 *Appl.* **13**, 1263–1275 (2003).
574 26. D. W. Weisrock, H. B. Shaffer, B. L. Storz, S. R. Storz, S. R. Voss, Multiple nuclear gene
575 sequences identify phylogenetic species boundaries in the rapidly radiating clade of
576 Mexican ambystomatid salamanders. *Mol. Ecol.* **15**, 2489–2503 (2006).
577 27. G. Parra-Olea, *et al.*, Conservation genetics of threatened Mexican axolotls (*Ambystoma*).
578 *Anim. Conserv.* **15**, 61–72 (2012).
579 28. E. Routman, Population structure and genetic diversity of metamorphic and paedomorphic
580 populations of the tiger salamander, *Ambystoma tigrinum*. *J. Evol. Biol.* **6**, 329–357
581 (1993).
582 29. R. Percino-Daniel, E. Recuero, E. Vázquez-Domínguez, K. R. Zamudio, G. Parra-Olea,
583 All grown-up and nowhere to go: Paedomorphosis and local adaptation in *Ambystoma*
584 salamanders in the Cuenca Oriental of Mexico. *Biol. J. Linn. Soc.* **118**, 582–597 (2016).
585 30. R. A. Brandon, Hybridization between the Mexican salamanders *Ambystoma dumerilii*

bioRxiv preprint doi: https://doi.org/10.1101/2020.07.10.197624; this version posted January 26, 2021. The copyright holder for this preprint (which was not certified by peer review) is the author/funder, who has granted bioRxiv a license to display the preprint in perpetuity. It is made available under aCC-BY-NC-ND 4.0 International license.

and *Ambystoma mexicanum* under laboratory conditions. *Herpetologica* **28**, 199–207 (1972).

31. R. A. Brandon, Interspecific hybridization among Mexican and United States salamanders of the genus *Ambystoma* under laboratory conditions. *Herpetologica* **33**, 133–152 (1977).

32. E. M. O'Neill, *et al*., Parallel tagged amplicon sequencing reveals major lineages and phylogenetic structure in the North American tiger salamander (*Ambystoma tigrinum*) species complex. *Mol. Ecol.* **22**, 111–129 (2013).

33. T. Jombart, S. Devillard, F. Balloux, Discriminant analysis of principal components: A new method for the analysis of genetically structured populations. *BMC Genet.* **11**, 94 (2010).

34. H. B. Shaffer, G. B. Pauly, J. C. Oliver, P. C. Trenham, The molecular phylogenetics of endangerment: Cryptic variation and historical phylogeography of the California tiger salamander, *Ambystoma californiense*. *Mol. Ecol.* **13**, 3033–3049 (2004).

35. D. H. Huson, SplitsTree: Analyzing and visualizing evolutionary data. *Bioinformatics* **14**, 68–73 (1998).

36. J. Chifman, L. Kubatko, Quartet inference from SNP data under the coalescent model. *Bioinformatics* **30**, 3317–3324 (2014).

37. A. J. Drummond, A. Rambaut, BEAST: Bayesian evolutionary analysis by sampling trees. *BMC Evol. Biol.* **7**, 214 (2007).

38. A. Stamatakis, RAxML version 8: A tool for phylogenetic analysis and post-analysis of large phylogenies. *Bioinformatics* **30**, 1312–1313 (2014).

39. A. A. Dugès, *Description d'un axolotl des montagnes de las cruces (*Amblystoma *[sic]* altamirani*, A. Dugès)* (Imprimerie du Ministère de "Fomento," 1895).

bioRxiv preprint doi: https://doi.org/10.1101/2020.07.10.197624; this version posted January 26, 2021. The copyright holder for this preprint (which was not certified by peer review) is the author/funder, who has granted bioRxiv a license to display the preprint in perpetuity. It is made available under aCC-BY-NC-ND 4.0 International license.

609 40. E. H. Taylor, Herpetological novelties from Mexico. *Univ. Kansas Sci. Bull.* **29**, 343–358
610 (1943).
611 41. E. H. Taylor, A new ambystomid salamander from the Plateau Region of Mexico. *Univ.*
612 *Kansas Sci. Bull.* **30**, 57–61 (1944).
613 42. S. Krebs, R. Brandon, A new species of salamander (family Ambystomatidae) from
614 Michoacan, Mexico. *Herpetologica* **40**, 238–245 (1984).
615 43. A. A. Dugès, Una nueva especie de ajolote de la Laguna de Patzcuaro. *La Nat.* **1**, 241–244
616 (1870).
617 44. J. Dixon, A new species of salamander of the genus Ambystoma from Jalisco, Mexico.
618 *Copeia* **1**, 99–101 (1963).
619 45. G. Shaw, F. Nodder, *The Naturalist's Miscellany; or Coloured Figures of Natural Objects*
620 *Drawn and Described Immediately from Nature*, 9th Ed. (Nodder & Co., 1798).
621 46. A. A. Dugès, Erpetología del valle de México. *La Nat.* **2**, 97–146 (1888).
622 47. J. R. Johnson, R. C. Thomson, S. J. Micheletti, H. B. Shaffer, The origin of tiger
623 salamander (*Ambystoma tigrinum*) populations in California, Oregon, and Nevada:
624 Introductions or relicts? *Conserv. Genet.* **12**, 355–370 (2011).
625 48. E. H. Taylor, Two new ambystomid salamanders from Chihuahua. *Copeia* **3**, 143–146
626 (1941).
627 49. R. Webb, Observations on tiger salamanders (*Ambystoma tigrinum* complex, family
628 Ambystomatidae) in Mexico with description of a new species. *Bull. Maryl. Herpetol.*
629 *Soc.* **40**, 122–143 (2004).
630 50. H. B. Shaffer, Biosystematics of *Ambystoma rosaceum* and *A. tigrinum* in Northwestern
631 Mexico. *Copeia* **1983**, 67 (1983).

bioRxiv preprint doi: https://doi.org/10.1101/2020.07.10.197624; this version posted January 26, 2021. The copyright holder for this preprint (which was not certified by peer review) is the author/funder, who has granted bioRxiv a license to display the preprint in perpetuity. It is made available under aCC-BY-NC-ND 4.0 International license.

632 51. R. A. Brandon, Spontaneous and induced metamorphosis of *Ambystoma dumerilii*
633 (Dugès), a paedogenetic Mexican salamander, under laboratory conditions. *Herpetologica*
634 **32**, 429–438 (1976).
635 52. H. M. Wilbur, J. P. Collins, Ecological aspects of amphibian metamorphosis: Nonnormal
636 distributions of competitive ability reflect selection for facultative metamorphosis. *Science*
637 **182**, 1305–1314 (1973).
638 53. R. M. Bonett, M. A. Steffen, S. M. Lambert, J. J. Wiens, P. T. Chippindale, Evolution of
639 paedomorphosis in plethodontid salamanders: Ecological correlates and re-evolution of
640 metamorphosis. *Evolution* **68**, 466–482 (2014).
641 54. C. R. Marshall, E. C. Raff, R. A. Raff, Dollo's law and the death and resurrection of
642 genes. *Proc. Natl. Acad. Sci. USA* **91**, 12283–12287 (1994).
643 55. M. J. West-Eberhard, Phenotypic plasticity and the origins of diversity. *Annu. Rev. Ecol.*
644 *Syst.* **20**, 249–278 (1989).
645 56. M. J. West-Eberhard, Alternative adaptations, speciation, and phylogeny (A Review).
646 *Proc. Natl. Acad. Sci. USA* **83**, 1388–92 (1986).
647 57. B. M. Fitzpatrick, Underappreciated consequences of phenotypic plasticity for ecological
648 speciation. *Int. J. Ecol.* **2012**, 1–12 (2012).
649 58. M. Denoël, P. Poncin, J.-C. Ruwet, Sexual compatibility between two heterochronic
650 morphs in the Alpine newt, *Triturus alpestris*. *Anim. Behav.* **62**, 559–566 (2001).
651 59. J. D. Krenz, P. A. Verrell, Integrity in the midst of sympatry: Does sexual incompatibility
652 facilitate the coexistence of metamorphic and paedomorphic mole salamanders
653 (*Ambystoma talpoideum*)? *J. Zool.* **258**, S0952836902001589 (2002).
654 60. H. H. Whiteman, J. D. Krenz, R. D. Semlitsch, Intermorph breeding and the potential for

bioRxiv preprint doi: https://doi.org/10.1101/2020.07.10.197624; this version posted January 26, 2021. The copyright holder for this preprint (which was not certified by peer review) is the author/funder, who has granted bioRxiv a license to display the preprint in perpetuity. It is made available under aCC-BY-NC-ND 4.0 International license.

reproductive isolation in polymorphic mole salamanders (*Ambystoma talpoideum*). *Behav. Ecol. Sociobiol.* **60**, 52–61 (2006).

61. H. Whiteman, J. Gutrich, R. Moorman, Courtship behavior in a polymorphic population of the tiger salamander, *Ambystoma tigrinum nebulosum*. *J. Herpetol.* **33**, 348–351 (1999).

62. R. D. Howard, R. S. Moorman, H. H. Whiteman, Differential effects of mate competition and mate choice on eastern tiger salamanders. *Anim. Behav.* **53**, 1345–1356 (1997).

63. D. H. Bos, R. N. Williams, D. Gopurenko, Z. Bulut, J. A. DeWoody, Condition-dependent mate choice and a reproductive disadvantage for MHC-divergent male tiger salamanders. *Mol. Ecol.* **18**, 3307–3315 (2009).

64. C. E. Nelson, R. R. Humphrey, Artificial interspecific hybridization among *Ambystoma*. *Herpetologica* **28**, 27–32 (1972).

65. S. R. Voss, H. B. Shaffer, Evolutionary genetics of metamorphic failure using wild-caught vs. laboratory axolotls (*Ambystoma mexicanum*). *Mol. Ecol.* **9**, 1401–1407 (2000).

66. S. R. Voss, K. L. Prudic, J. C. Oliver, H. B. Shaffer, Candidate gene analysis of metamorphic timing in ambystomatid salamanders. *Mol. Ecol.* **12**, 1217–1223 (2003).

67. J. B. Armstrong, G. M. Malacinski, *Developmental Biology of the Axolotl* (Oxford University Press, 1989).

68. J. M. Velasco, Anotaciones y observaciones al trabajo del Sr. D. A. Weismann sobre la transformación del ajolote Mexicano en Amblistoma. *La Nat.* **5**, 58–84 (1880).

69. H. M. Smith, The Mexican axolotl: Some misconceptions and problems. *Bioscience* **19**, 593–615 (1969).

70. L. L. Bailey, T. R. Simons, K. H. Pollock, Estimating site occupancy and species detection probability parameters for terrestrial salamanders. *Ecol. Appl.* **14**, 692–702

bioRxiv preprint doi: https://doi.org/10.1101/2020.07.10.197624; this version posted January 26, 2021. The copyright holder for this preprint (which was not certified by peer review) is the author/funder, who has granted bioRxiv a license to display the preprint in perpetuity. It is made available under aCC-BY-NC-ND 4.0 International license.

(2004).

71. C. L. Morjan, L. H. Rieseberg, How species evolve collectively: Implications of gene flow and selection for the spread of advantageous alleles. *Mol. Ecol.* **13**, 1341–1356 (2004).

72. J. McKay, "An evaluation of captive breeding and sustainable use of the Mexican axolotl (*Ambystoma mexicanum*)," University of Kent, Canterbury, UK. (2003) (January 20, 2020).

73. J. L. Tamayo, R. C. West, "The hydrography of middle America" in *Handbook of Middle American Indians*, R. Wauchope, R. C. West, Eds. (University of Texas Press, 1964), pp. 84–121.

74. G. R. Hopkins, E. D. Brodie, Occurrence of amphibians in saline habitats: A review and evolutionary perspective. *Herpetol. Monogr.* **29**, 1–27 (2015).

75. K. De Queiroz, Species concepts and species delimitation. *Syst. Biol.* **56**, 879–886 (2007).

76. P. M. Hime, *et al.*, Phylogenomics reveals ancient gene tree discordance in the amphibian tree of life. *Syst. Biol.* (2020) https:/doi.org/10.1093/sysbio/syaa034 (May 12, 2020).

77. J. Koster, S. Rahmann, Snakemake: A scalable bioinformatics workflow engine. *Bioinformatics* **28**, 2520–2522 (2012).

78. A. M. Bolger, M. Lohse, B. Usadel, Trimmomatic: A flexible trimmer for Illumina sequence data. *Bioinformatics* **30**, 2114–2120 (2014).

79. H. Li, A statistical framework for SNP calling, mutation discovery, association mapping and population genetical parameter estimation from sequencing data. *Bioinformatics* **27**, 2987–2993 (2011).

80. E. Garrison, G. Marth, Haplotype-based variant detection from short-read sequencing. *arXiv* **1207.3907** (2012).

bioRxiv preprint doi: https://doi.org/10.1101/2020.07.10.197624; this version posted January 26, 2021. The copyright holder for this preprint (which was not certified by peer review) is the author/funder, who has granted bioRxiv a license to display the preprint in perpetuity. It is made available under aCC-BY-NC-ND 4.0 International license.

81. P. Danecek, *et al*., The variant call format and VCFtools. *Bioinformatics* **27**, 2156–2158 (2011).

82. M. Martin, *et al*., WhatsHap: Fast and accurate read-based phasing. *bioRxiv* **10.1101/08** (2016).

83. K. Katoh, D. M. Standley, MAFFT multiple sequence alignment software version 7: Improvements in performance and usability. *Mol. Biol. Evol.* **30**, 772–780 (2013).

84. A. J. Page, *et al*., SNP-sites: Rapid efficient extraction of SNPs from multi-FASTA alignments. *Microb. genomics* **2**, e000056 (2016).

85. R Core Team, R: a language and environment for statistical computing (2012).

86. T. Jombart, adegenet: A R package for the multivariate analysis of genetic markers. *Bioinformatics* **24**, 1403–1405 (2008).

87. T. Jombart, C. Collins, A tutorial for discriminant analysis of principal components (DAPC) using adegenet 2.0. 0. *adegenet.r-forge.r-project.org* (2015) (May 30, 2019).

88. J. K. J. Pritchard, M. Stephens, P. Donnelly, Inference of population structure using multilocus genotype data. *Genetics* **155**, 945–959 (2000).

89. G. Evanno, S. Regnaut, J. Goudet, Detecting the number of clusters of individuals using the software structure: A simulation study. *Mol. Ecol.* **14**, 2611–2620 (2005).

90. N. M. Kopelman, J. Mayzel, M. Jakobsson, N. A. Rosenberg, I. Mayrose, Clumpak: A program for identifying clustering modes and packaging population structure inferences across K. *Mol. Ecol. Resour.* **15**, 1179–1191 (2015).

91. D. H. Huson, D. Bryant, Application of phylogenetic networks in evolutionary studies. *Mol. Biol. Evol.* **23**, 254–267 (2006).

92. D. Bryant, V. Moulton, Neighbor-Net: An agglomerative method for the construction of

bioRxiv preprint doi: https://doi.org/10.1101/2020.07.10.197624; this version posted January 26, 2021. The copyright holder for this preprint (which was not certified by peer review) is the author/funder, who has granted bioRxiv a license to display the preprint in perpetuity. It is made available under aCC-BY-NC-ND 4.0 International license.

724 phylogenetic networks. *Mol. Biol. Evol.* **21**, 255–265 (2003).

725 93. A. Rambaut, A. Drummond, D. Xie, G. Baele, M. Suchard, Tracer v1.7 (2018).

726 94. J. Sukumaran, M. Holder, DendroPy: A Python library for phylogenetic computing.

727 *Bioinformatics* **26**, 1569–1571 (2010).

728 95. R. Lanfear, B. Calcott, S. Y. W. Ho, S. Guindon, PartitionFinder: Combined selection of

729 partitioning schemes and substitution models for phylogenetic analyses. *Mol Biol Evol* **29**,

730 1695–1701 (2012).

731 96. M. A. Miller, W. Pfeiffer, T. Schwartz, Creating the CIPRES Science Gateway for

732 inference of large phylogenetic trees in *2010 Gateway Computing Environments*

733 *Workshop (GCE)*, (IEEE, 2010), pp. 1–8.

734 97. D. Swofford, PAUP 4.0 b10: Phylogenetic analysis using parsimony (2002) (December

735 21, 2013).

736 98. A. Rambaut, FigTree, a graphical viewer of phylogenetic trees (2007) (May 8, 2014).

737 99. P. Beerli, M. Palczewski, Unified framework to evaluate panmixia and migration direction

738 among multiple sampling locations. *Genetics* **185**, 313–326 (2010).

739 100. C. Aktas, Haplotypes: Haplotype inference and statistical analysis of genetic variation

740 (2015).

741 101. D. Nychka, R. Furrer, J. Paige, S. Sain, fields: Tools for spatial data (2017).

742 102. P. Dixon, VEGAN, a package of R functions for community ecology. *J. Veg. Sci.* **14**,

743 927–930 (2003).

744

bioRxiv preprint doi: https://doi.org/10.1101/2020.07.10.197624; this version posted January 26, 2021. The copyright holder for this preprint (which was not certified by peer review) is the author/funder, who has granted bioRxiv a license to display the preprint in perpetuity. It is made available under aCC-BY-NC-ND 4.0 International license.

Figure Legends

Figure 1. Discriminant analysis of principal components (DAPC) on (A) the entire genomic dataset (without *A. opacum* and *A. texanum* outgroups), and (B) the genomic dataset without *A. californiense*. In both analyses, patterns of genetic differentiation stabilized at values of $K \geq 5$ ($K = 5$ is shown in both plots, with colors representing genetic clusters). Points represent individuals and ellipses show the groups identified by DAPC. The first and second principal components from the DAPC are on the x and y axes, respectively. Results from additional values of K are provided in Supplementary Figures 3 and 4.

Figure 2. Population genomic analyses of the *Ambystoma tigrinum* species complex. (A) STRUCTURE plot of central Mexico samples. While the Evanno et al. (2005) method identified $K = 7$, four major geographic genetic groups are apparent and were analyzed separately in subsequent analyses (B-E). In each plot, vertical bars represent individuals, while the y-axis shows the membership probability for each group. Pie charts mapped below the assignment plot show the average group membership probability for that locality. Some localities were combined to a single pie chart to reduce visual clutter; see Table S1 for specific coordinates of each sample. The range of the Trans-Mexican Volcanic Belt (TMVB) is identified by shading and is modified from Ferrari (2004). The range of the Cuenca Oriental is outlined in red and is modified from Percino-Daniel et al. (2016). Two geographic outliers placed in CM2 are thought to represent range introductions and are not shown here, but are discussed in supplementary text and shown in Fig. S9. (F,G) STRUCTURE results from analyses of the U.S. and northern Mexico groups, respectively. Detailed results are shown in Figs. S11-S12. Black squares on the maps denote the type localities of all species included in this study. On each STRUCTURE membership plot, salamander face symbols denote the presence of salamanders with a life history category of 1-3 (the cartoon lacks gills) or 4-5 (paedomorphic, cartoon shows gills); groups labeled with both symbols contain a mixture of these life history categories.

Figure 3. Results of phylogenetic network analyses (left) and the SVDquartets-based species tree analysis (right) of the *Ambystoma tigrinum* species complex. Clades are colored according to their cluster assignments in population genetic analyses, as in Fig. 2. In phylogenetic networks, species names are only shown for paedomorphic taxa in categories 4 or 5 (Table 1). Life history categories for all taxa are given in parentheses in the species tree. Note that SVDquartet analysis used a subset of individuals, indicated by solid circles on the phylogenetic networks. Phylogenetic results from Bayesian and maximum-likelihood concatenated analyses were largely concordant with the quartets tree (Fig. S13), although two important differences are indicated by dashed lines. Bootstrap support (BS) values are indicated on each node of the quartets tree (BS values ≥ 95 are not shown), while tips are labeled with individual IDs (Table S1). Branch lengths are not scaled to time or substitution rate.

Figure 4. Maps (left) show localities for CM3 and CM4, the two genetic clusters containing paedomorphic taxa (life history categories 4 and 5). The top-ranked migration model is shown to the right of each map, with median mutation-scaled effective population sizes (Θ) shown inside the shapes denoting populations. Arrows indicate the direction of migration ($M = m/\mu$, where m is the fraction of immigrants in each generation and μ is the mutation rate per generation per site) and median migration rates are provided next to each arrow. Full model test results are provided

bioRxiv preprint doi: https://doi.org/10.1101/2020.07.10.197624; this version posted January 26, 2021. The copyright holder for this preprint (which was not certified by peer review) is the author/funder, who has granted bioRxiv a license to display the preprint in perpetuity. It is made available under aCC-BY-NC-ND 4.0 International license.

in Table S3 and full parameter estimates are provided in Table S4. Scatterplots (right) show pairwise geographic distances by pairwise ϕ_{ST} among all populations. Point colors and shapes denote the life history strategies of the pairwise comparison being made: black squares = both populations are facultatively paedomorphic; red circles = one population is facultatively paedomorphic and one population is obligately paedomorphic; black stars = both populations are obligately paedomorphic. Solid lines denote the line of best fit, calculated separately for each life history comparison. Regressions were not performed on paedomorph-paedomorph comparisons due to low sample sizes. Shaded areas denote the 95% confidence interval for the regression. P-values to the right of each graph were calculated using a partial mantel test, which tested for a correlation between ϕ_{ST} and life history while correcting for geographic distance (n.s. = not significant).

Table 1. Currently recognized species in the *Ambystoma tigrinum* complex. Habitat preference, range, conservation status ("Status"), and life history strategy were compiled from AmphibiaWeb (2019) and the IUCN (2019). Conservation status abbreviations: LC = least concern, V = vulnerable, E = endangered, CE = critically endangered, DD = data deficient. Life history codes: 1 = obligate metamorph (no paedomorphs documented in the field), 2 = Strong bias towards metamorphosis with rare paedomorphs found in the field, 3 = Both metamorphosis and paedomorphosis common in the field, 4 = Strong bias towards paedomorphosis with rare metamorphs found in the field, 5 = obligate paedomorph (no metamorphs documented in the field). In the text, "paedomorph" describes taxa scored as 4 or 5, while "facultative paedomorph" describes taxa scored as 2 or 3.

Species	Habitat Preference	Range	Status	Life History
Ambystoma altamirani Dugès, 1895	Streams, occasional ponds	High elevations in the west and south of the Valley of Mexico (Mexico State, Morelos, and Distrito Federal)	E	2
Ambystoma amblycephalum Taylor, 1940	Ponds	Small area of Tacicuaro (north and west Michoacan)	CE	2
Ambystoma andersoni Krebs & Brandon, 1984	Lakes / Ponds	Restricted to Lake Zacapu and its outflow streams (north-central Michoacan)	CE	5
Ambystoma bombypellum Taylor, 1940	Lakes / Ponds, occasional streams	Known only from type locality San Martin/Asunción, 15 km west of Morelia (Michoacan)	DD	2
Ambystoma californiense Gray 1853	Vernal pools	Great Central Valley and adjacent inner coast ranges, central California	V	1
Ambystoma dumerilii (Dugès, 1870)	Lakes / Ponds	Restricted to Lake Patzcauro (north-central Michoacan)	CE	5
Ambystoma flavipiperatum Dixon, 1963	Lakes / Ponds, occasional streams	Sierra de Quila (Jalisco). Historically known from the type locality in Santa Cruz, southwest of Guadalajara.	E	3
Ambystoma granulosum Taylor, 1944	Lakes / Ponds, occasional streams	Northwest of Toluca city (Mexico State and border of Michoacan)	CE	3
Ambystoma leorae (Taylor, 1943)	Streams	High elevations of Rio Frio in Iztaccihuatl -Popocatepetl Natl. Park (Mexico State and adjacent Puebla)	CE	2
Ambystoma lermaense (Taylor, 1940)	Lakes / Ponds	Highlands near Toluca, in Rio Lerma and Lake Lerma near Almoloya (Mexico State)	E	3
Ambystoma mavortium Baird, 1850*	Lakes / Ponds	Widespread distribution from west-central Canada through the USA to northern Mexico (Sonora, Chihuahua, Coahuila). Disjunct distribution in northwestern USA and Canada (Washington, British Columbia).	LC	3
Ambystoma mexicanum (Shaw and Nodder, 1798)	Lakes	Southern areas of Xochimilco (Mexico City). Historically distributed in Lakes of Xochimilco and Chalco.	CE	4
Ambystoma ordinarium Taylor, 1940	Streams	From south of Patzcuaro through Morelia City to eastern Michoacan	E	3
Ambystoma rivulare (Taylor, 1940)	Streams	Sierra Chinchua, Mariposa Monarca Biosphere Reserve, Michoacan, Valle de Bravo, Amanalco and Nevado de Toluca (Mexico State)	E	2
Ambystoma rosaceum Taylor, 1941	Streams	Sierra Madre Occidental (Sonora, Durango, Chihuahua, Sinaloa, Nayarit, Jalisco)	LC	3
Ambystoma silvense Webb, 2004	Lakes / Ponds	Sierra Madre Occidental (at least Chihuahua, Durango)	DD	3
Ambystoma taylori Brandon et al., 1982	Saline lake	Restricted to Lake Alchichica (Puebla)	CE	4
Ambystoma tigrinum Green, 1825	Lakes / Ponds	From southeast Canada south to east Texas and extending east of the Appalachian Mountains through the Atlantic Coastal Plain north to Long Island (New York)	LC	2
Ambystoma velasci (Dugès, 1888)	Lakes / Ponds, Streams	Sierra Madre Occidental (Chihuahua) and south across central Mexico (Durango, Jalisco, Nuevo León, Coahuila, Zacatecas, San Luis Potosi, Hidalgo, Queretaro, Tlaxcala, Puebla, Veracruz, Aguascalientes)	LC	3

bioRxiv preprint doi: https://doi.org/10.1101/2020.07.10.197624; this version posted January 26, 2021. The copyright holder for this preprint (which was not certified by peer review) is the author/funder, who has granted bioRxiv a license to display the preprint in perpetuity. It is made available under aCC-BY-NC-ND 4.0 International license.

bioRxiv preprint doi: https://doi.org/10.1101/2020.07.10.197624; this version posted January 26, 2021. The copyright holder for this preprint (which was not certified by peer review) is the author/funder, who has granted bioRxiv a license to display the preprint in perpetuity. It is made available under aCC-BY-NC-ND 4.0 International license.

A) DAPC of full dataset

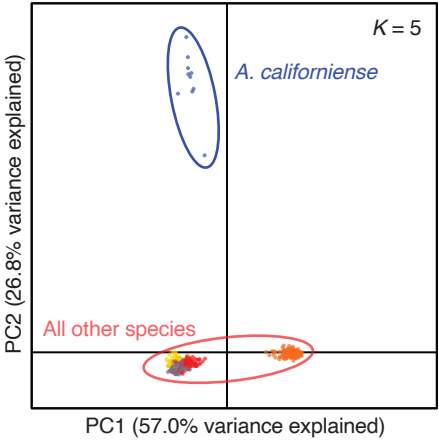

B) DAPC without *A. californiense*

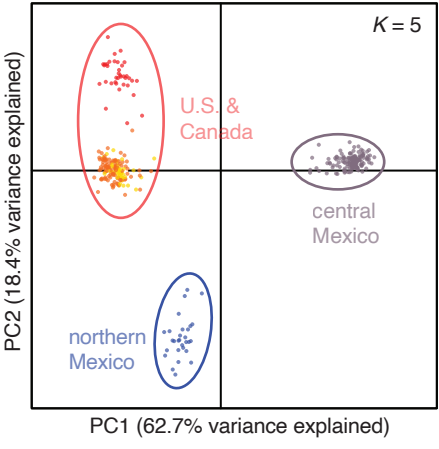

bioRxiv preprint doi: https://doi.org/10.1101/2020.07.10.197624; this version posted January 26, 2021. The copyright holder for this preprint (which was not certified by peer review) is the author/funder, who has granted bioRxiv a license to display the preprint in perpetuity. It is made available under aCC-BY-NC-ND 4.0 International license.

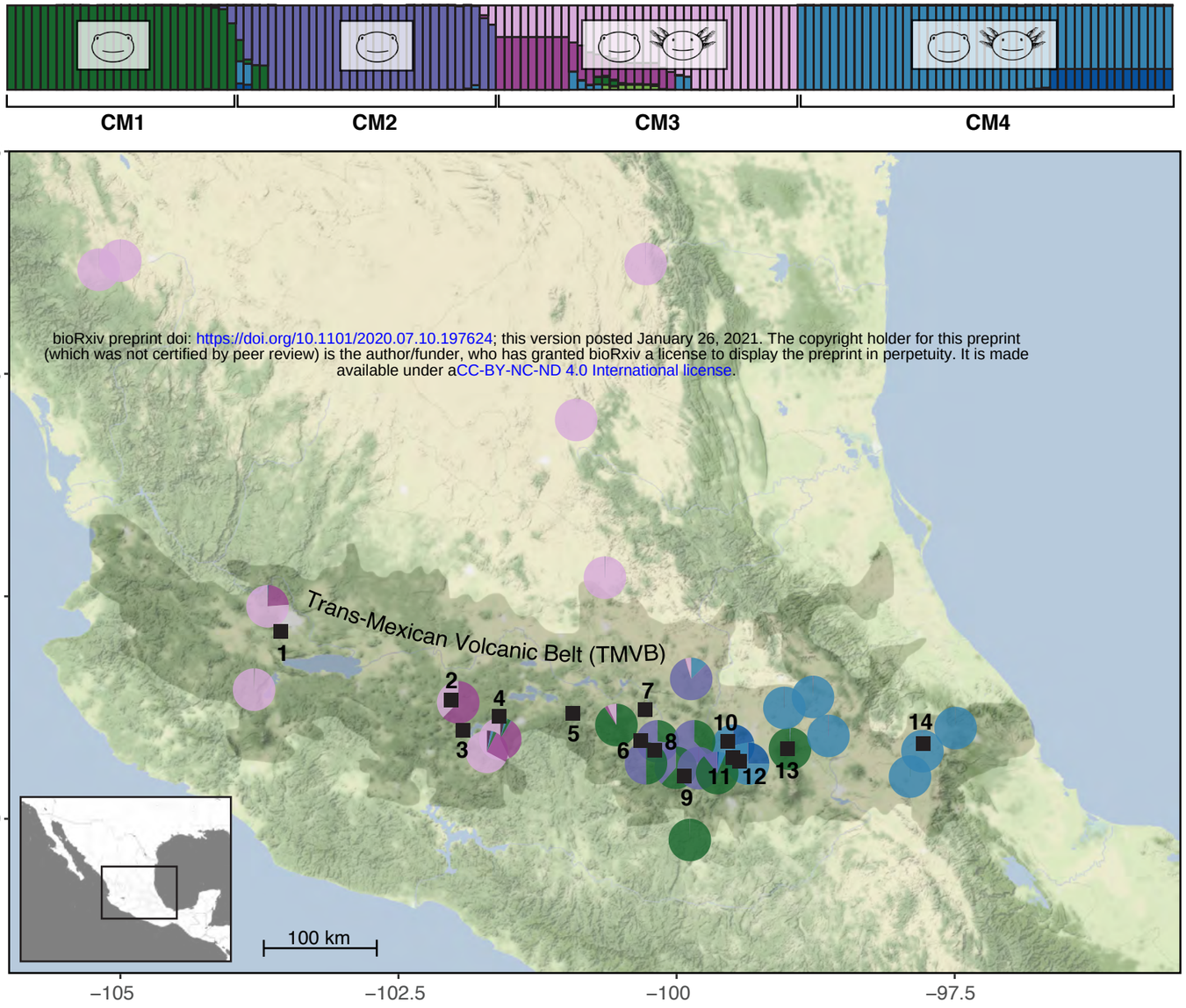

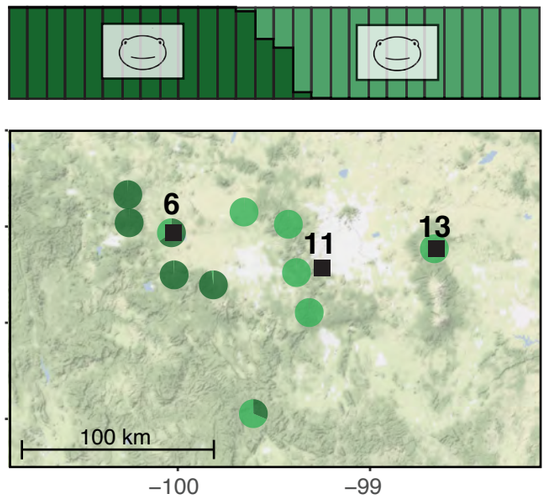

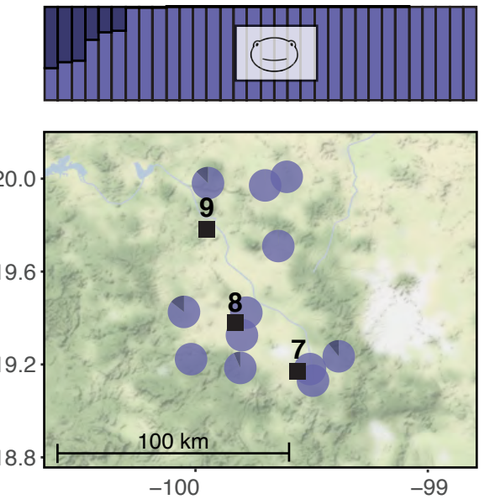

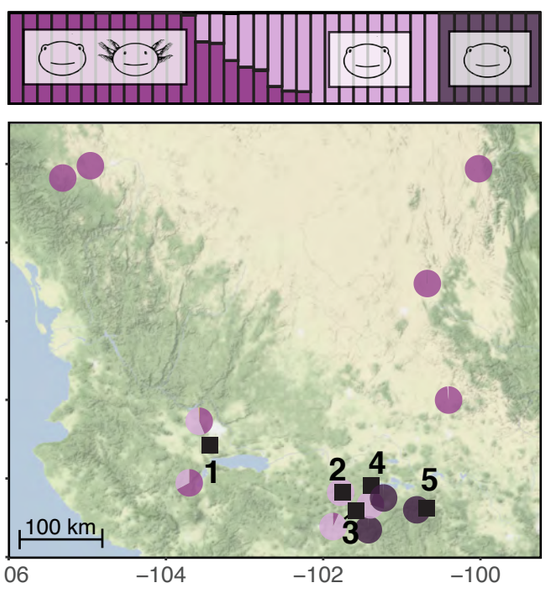

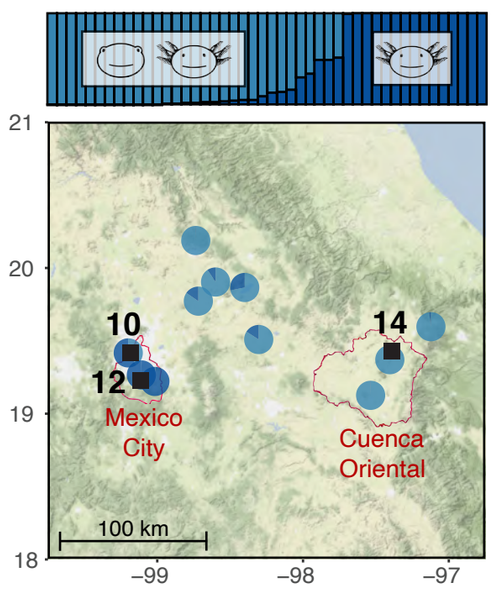

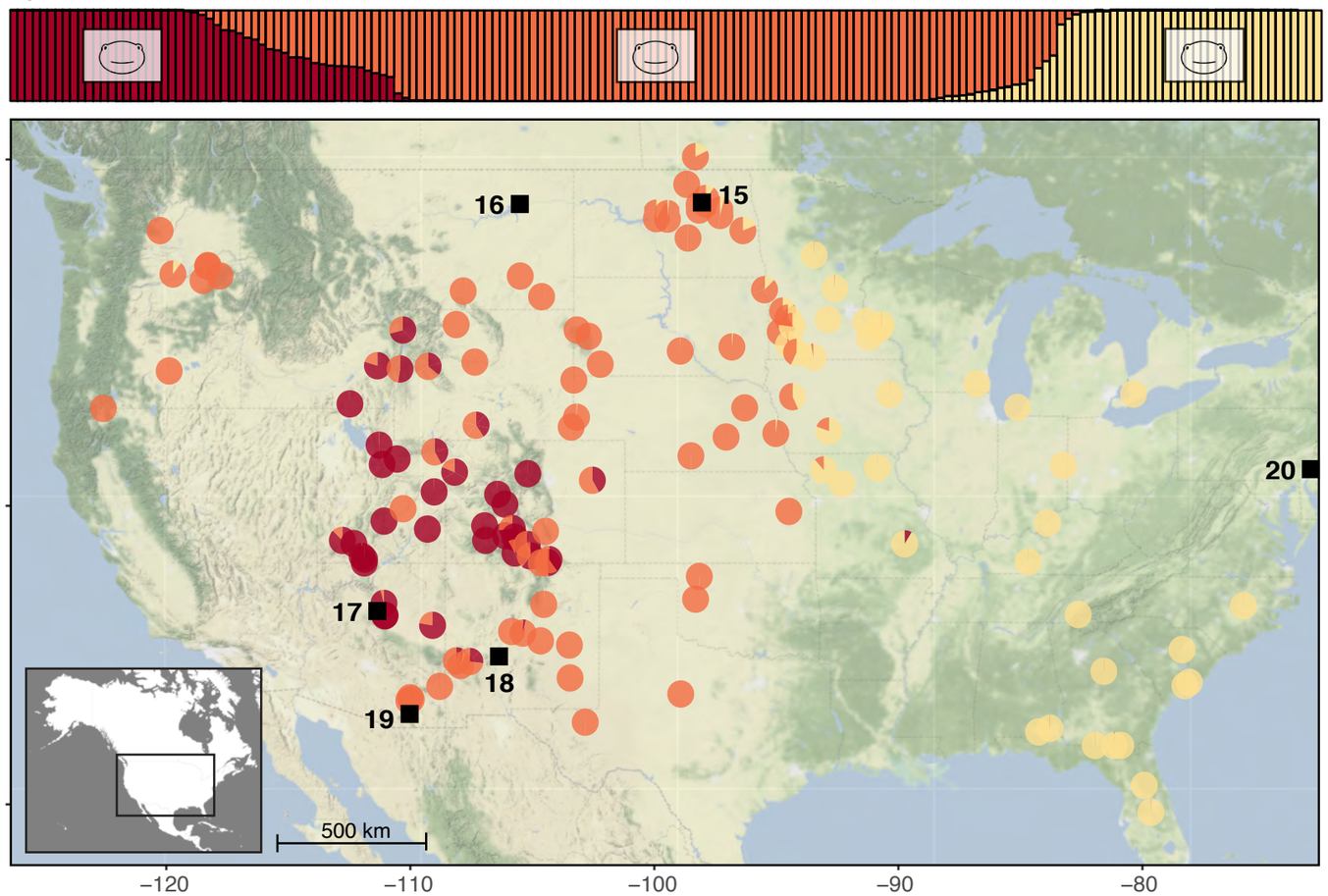

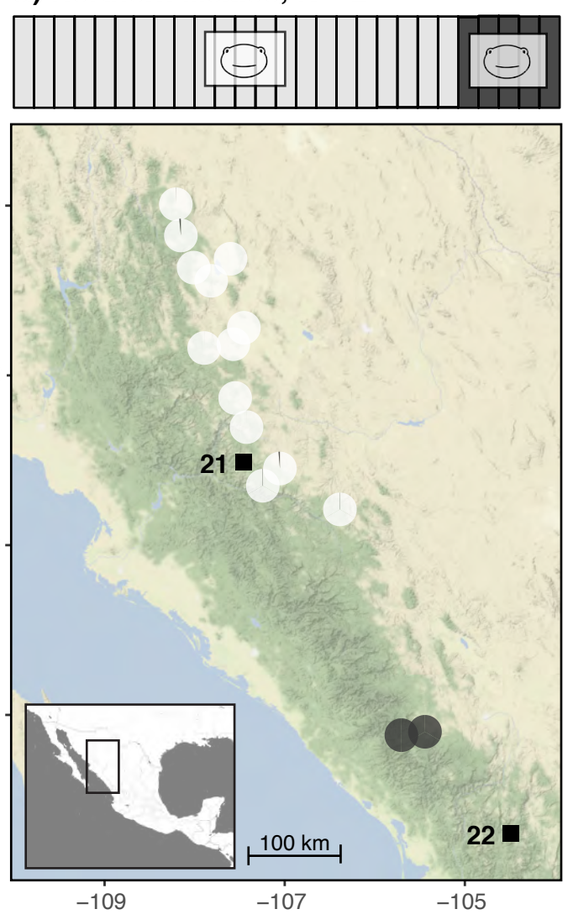

Type Localities (■)

1) *Ambystoma flavipiperatum*
2) *A. andersoni*
3) *A. dumerilii*
4) *A. amblycephalum*
5) *A. ordinarium*
6) *A. rivulare*
7) *A. bombypellum*
8) *A. granulosum*
9) *A. lermaense*
10) *A. velasci*
11) *A. altamirani*
12) *A. mexicanum*
13) *A. leorae*
14) *A. taylori*
15) *A. mavortium diaboli*
16) *A. m. melanostictum*
17) *A. m. nebulosum*
18) *A. m. mavortium*
19) *A. m. stebbinsi*
20) *A. tigrinum tigrinum*
21) *A. rosaceum*
22) *A. silvense*

Paedomorph (category 4 or 5)

Facultative Paedomorph/ Metamorph (categories 1-3)

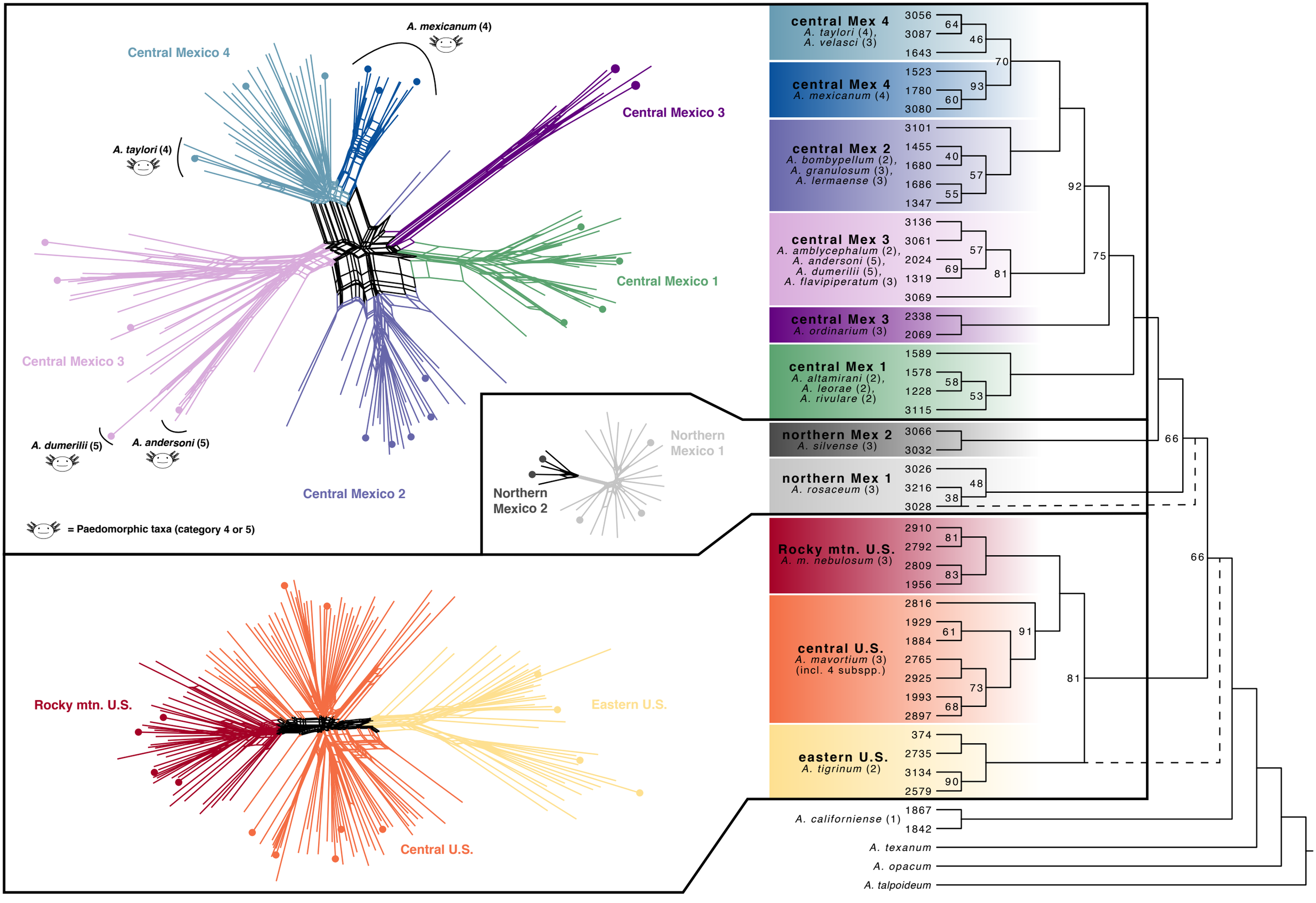
A. mexicanum (4)
Central Mexico 4
Central Mexico 3
A. taylori (4)
Central Mexico 1
Central Mexico 3
A. dumerilii (5)
A. andersoni (5)
Central Mexico 2
= Paedomorphic taxa (category 4 or 5)
Northern Mexico 1
Northern Mexico 2
Rocky mtn. U.S.
Eastern U.S.
Central U.S.
central Mex 4
A. taylori (4), A. velasci (3)
3056
3087
1643
central Mex 4
A. mexicanum (4)
1523
1780
3080
central Mex 2
A. bombypellum (2), A. granulosum (3), A. lermaense (3)
3101
1455
1680
1686
1347
central Mex 3
A. amblycephalum (2), A. andersoni (5), A. dumerilii (5), A. flavipiperatum (3)
3136
3061
2024
1319
3069
central Mex 3
A. ordinarium (3)
2338
2069
central Mex 1
A. altamirani (2), A. leorae (2), A. rivulare (2)
1589
1578
1228
3115
northern Mex 2
A. silvense (3)
3066
3032
northern Mex 1
A. rosaceum (3)
3026
3216
3028
Rocky mtn. U.S.
A. m. nebulosum (3)
2910
2792
2809
1956
central U.S.
A. mavortium (3) (incl. 4 subspp.)
2816
1929
1884
2765
2925
1993
2897
eastern U.S.
A. tigrinum (2)
374
2735
3134
2579
A. californiense (1)
1867
1842
A. texanum
A. opacum
A. talpoideum
64
46
70
93
60
40
57
55
92
57
69
81
75
58
53
66
48
38
81
83
66
91
61
73
68
90
81

Central Mexico Group 3 (CM3)

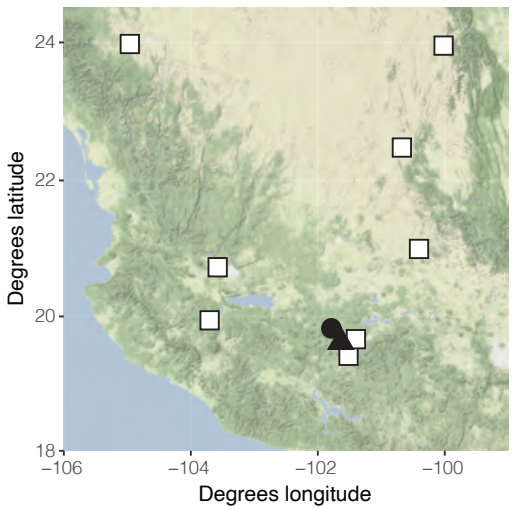

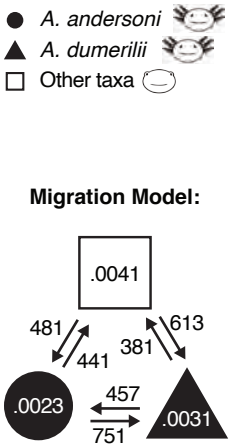

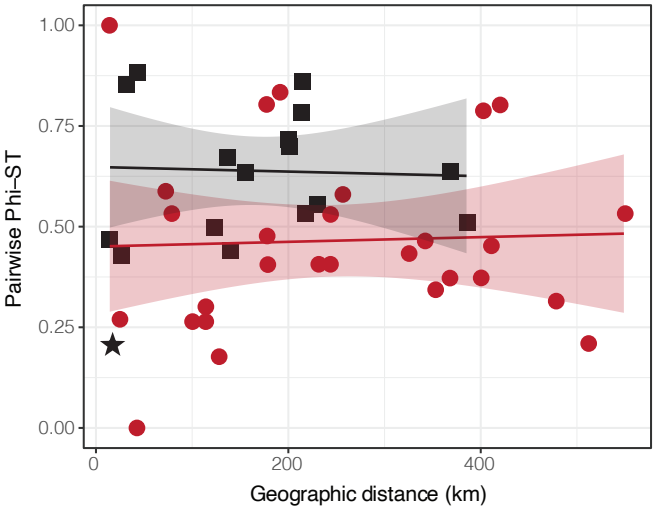

Population pair
- Facultative-Facultative
- Facultative-Paedomorph
- Paedomorph-Paedomorph

Partial Mantel Statistic: -0.158
p-value = 0.791 (n.s.)

Central Mexico Group 4 (CM4)

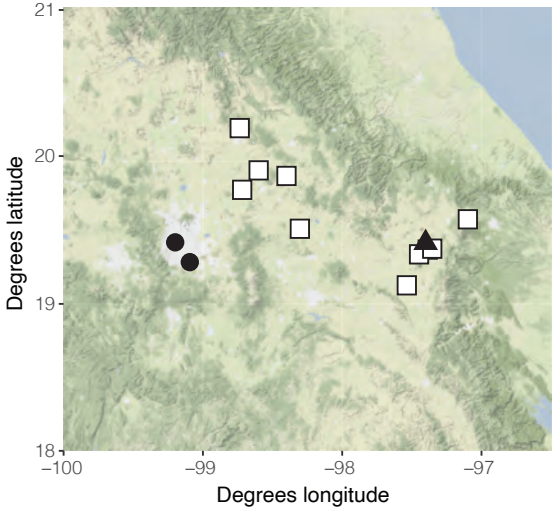

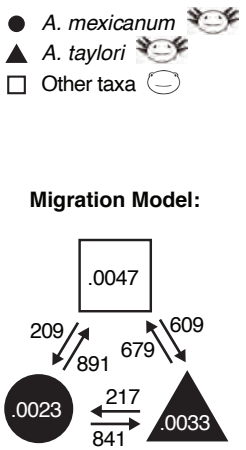

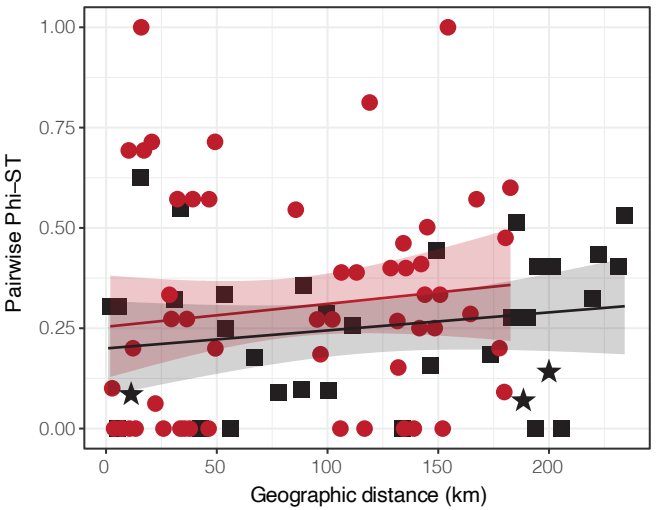

Population pair
- Facultative-Facultative
- Facultative-Paedomorph
- Paedomorph-Paedomorph

Partial Mantel Statistic: 0.245
p-value = 0.18 (n.s.)